WARSAW UNIVERSITY OF TECHNOLOGY Index 351733
FACULTY OF CIVIL ENGINEERING
COMMITTEE FOR CIVIL AND WATER ENGINEERING
POLISH ACADEMY OF SCIENCES ISSN 1230-2945

DOI: 10.24425/ace.2023.144159

ARCHIVES OF CIVIL ENGINEERING

Vol. LXIX ISSUE 1 2023

© 2023. Michał Gołdyn.

pp. 55 – 70

This is an open-access article distributed under the terms of the Creative Commons Attribution-NonCommercial-NoDerivatives License (CC BY-NC-ND 4.0, https://creativecommons.org/licenses/by-nc-nd/4.0/), which permits use, distribution, and reproduction in any medium, provided that the Article is properly cited, the use is non-commercial, and no modifications or adaptations are made.

Review paper

Application of the Critical Shear Crack Theory for calculation of the punching shear capacity of lightweight aggregate concrete slabs

Michał Gołdyn[1]

Abstract: The paper discusses the principles of the Critical Shear Crack Theory (CSCT) in terms of the punching shear analysis of flat slabs made from lightweight aggregate concretes. The basic assumptions of the CSCT were discussed, explaining the differences with regard to the calculation of ordinary concrete flat slabs, relating mainly to the adopted failure criterion associated with ultimate slab rotation. Taking into account the observations and conclusions from the previous experimental investigations, it was confirmed, that contribution of lightweight aggregate particles in the aggregate interlock effect should be ignored, due to possibility of aggregate breaking. However, the analysis of the profile of failure surface confirmed, that particles of the natural fine aggregate increase the roughness of the surface and should be included by formulating failure criterion for LWAC slabs.

The theoretical load-rotation relationships were compared with the results of measurements, confirming good agreement in most cases. The theoretical ultimate rotations were lower on average by about 11% than the experimental ones. The analysis of 57 results of the experimental investigations on punching shear of LWAC slabs made from various types of artificial aggregates showed a very good agreement with predictions of the CSCT. The obtained ratio of the experimental to theoretical load was 1.06 with a coefficient of variation of 9.1%. The performed parametric study demonstrated a low sensitivity of the correctness of the CSCT predictions to a change in a fairly wide range of parameters such as: the longitudinal reinforcement ratio, concrete compressive strength and concrete density.

Keywords: punching shear, lightweight aggregate concrete, aggregate interlock, particle size, Critical Shear Crack Theory

[1]PhD., Eng., Lodz University of Technology, Department of Concrete Structures, al. Politechniki 6, 93-590 Łódź, Poland, e-mail: michal.goldyn@p.lodz.pl, ORCID: 0000-0002-7791-1940

www.czasopisma.pan.pl PAN www.journals.pan.pl

1. Introduction

One of the most important considerations when designing flat slabs is analysis of the punching shear resistance within support zones. This issue becomes particularly important in case of structures made of lightweight aggregate concretes (LWAC), which, despite their undoubted advantages, such as lower specific gravity or better insulation properties, are characterized by lower tensile strength compared to ordinary concretes of similar compressive strength. Depending on the type of lightweight aggregate used, this difference reaches from about 10 to even more than 30% [1–3]. Contrary to the existing standard EN 1992-1-1 [4] which includes semi-empirical formulas for calculating the punching shear resistance, in *fib* Model Code 2010 [5] and prEN 1992-1-1 [6] procedures the mechanical approach according to the Critical Shear Crack Theory (CSCT) was adopted. According to this theory, the tangential crack, initially formed as a result of bending, transforms into an shear crack due to the action of shear forces and gradually propagates inside the slab. Formation of this diagonal crack disrupts direct transmission of forces through the concrete strut [7]. Then, the mechanism of shear transfer becomes dependent on the aggregate interlock effect, the residual tensile strength of the concrete, the shear band mechanism and the dowel action of the longitudinal reinforcement [8]. The punching shear resistance is related to deformation capacity, expressed in case of slender slabs by the rotation ψ. The load carrying capacity was expressed as the point of intersection of the curves describing load-deformation relationship (red line) and the failure criterion corresponding to punching shear (black line) – Fig. 1.

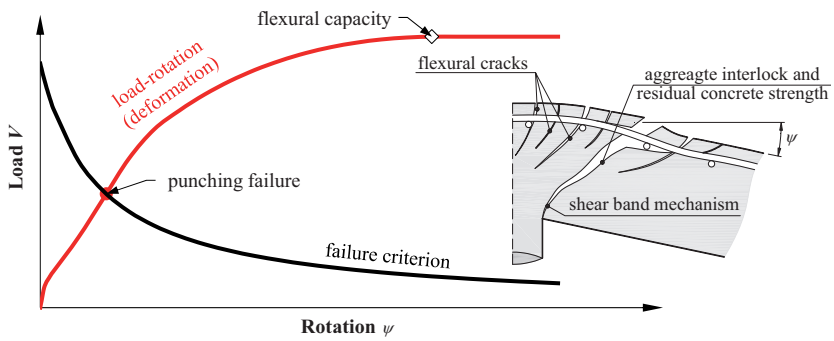

Fig. 1. Determination of the punching shear capacity according to the CSCT principles

2. Theoretical principles of the CSCT

2.1. Load-rotation response

In the support zones of flat slabs it comes to a concentration of forces resulting from bending and shear. Taking into account the previous conclusions of *Kinnunen* and *Nylander* [9], in the physical model adopted in the CSCT, the slab rotation ψ was assumed as

a parameter describing the deformations in the shear zone, which can be expressed as the integral of the slab curvature in this area. The analytical load-deformation relationship was developed on basis of the equilibrium conditions of the separated slab segment, assuming the moment-curvature relationship describing the slab behaviour. For design purposes, *Muttoni* [7] proposed a simplified equation expressing the relationship between load V and slab rotation ψ. After transformations, this function can be expressed in the following form

$$V(\psi) = \min \left\{ \begin{array}{c} \left(\psi \dfrac{1}{k_m} \dfrac{d}{r_s} \dfrac{E_s}{f_y} \right)^{\frac{2}{3}} \\ 1.0 \end{array} \right\} V_{\text{flex}} \tag{2.1}$$

where: ψ – the slab rotation, k_m – factor equal to 1.2 for refined estimation of the physical parameters and 1.5 in general case, d – the effective depth, r_s – the distance between line of contraflexure and axis of the column, E_s – the modulus of elasticity, f_y – the yield strength, V_{flex} – the flexural capacity.

The fib Model Code 2010 [5] procedure does not clearly distinguish the principles of punching shear design of lightweight aggregate concrete slabs, as is in case of the existing standard EN 1992-1-1 [4], in which additional reduction factors, depending on the concrete density, were introduced. Lightweight structural concretes of 1.8 and 2.0 density classes are characterized by a modulus of elasticity lower by about 20÷30% than ordinary concretes with the same compressive strength. The procedure [5] assumes that the deformations of a cracked slab are primarily related to the cross-section and the longitudinal reinforcement. Thus, the equation (2.1) should describe load-rotation of both ordinary and lightweight aggregate concrete slabs. This assumption seems to be confirmed by the results of the experimental investigations on flat slabs with the same shape and reinforcement, but made from different concretes. Figure 2 shows the experimental load-deflection curves

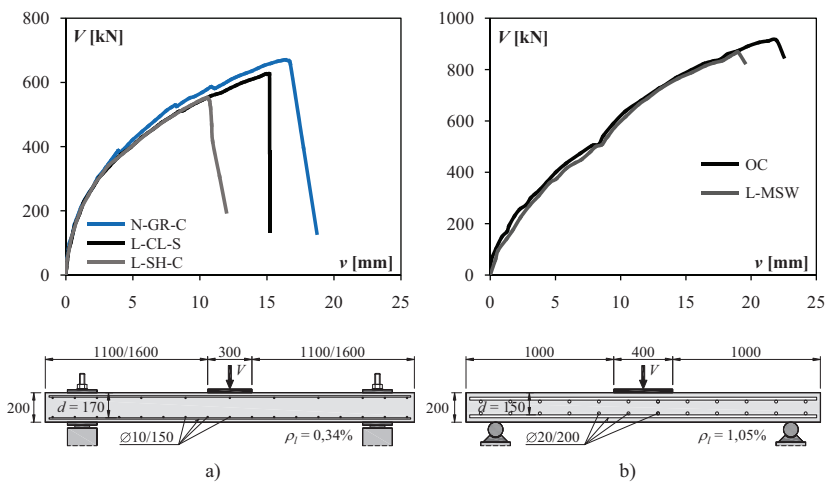

Fig. 2. Comparison between deflections of the slabs from ordinary and lightweight aggregate concrete: a) results from [10], b) results from [11]

describing behaviour of slabs considered in the study of *Youm* et al. [10]. The specimens with a thickness of 200 mm and a relatively low reinforcement ratio $\rho_l = 0.34\%$ were made from ordinary concrete with crushed granite aggregate (N-GR-C), lightweight concrete with shale coarse aggregates with crushed shapes (L-SH-C) and lightweight concrete with clay coarse aggregates with spherical shapes (L-CL-S). The concretes were characterized by a compressive strength of 34.2÷40.6 MPa. It can be seen that the course of the curves is similar, although deflection of the ordinary concrete slab at the same load level was on average about 10% lower. The results of measurements carried out by *Caratelli* et al. [11], including slabs from ordinary concrete (OC) and concrete with the addition of expanded clay aggregate (0÷15 mm) replacing about 75% of natural coarse aggregate (L-MSW), characterized by the same reinforcement ratio $\rho_l = 1.05\%$ and almost identical concrete compressive strength $f_{\mathrm{cm}} = 57.6 \div 58.6$ MPa, also indicate similar behaviour of both elements.

2.2. Failure criterion

The failure criterion is described by a semi-empirical formula, which combines the punching shear capacity with width of the diagonal crack related to the slab rotation ψ. The original equation introduced by *Muttoni* and *Schwartz* [12] has been modified in order to account for effect of the aggregate on the punching shear resistance. The size of the particles affects the roughness of the failure surface. Therefore, with the same crack width, a more pronounced effect of aggregate interlock, responsible for the transfer of shear stress, should be expected in case of concrete containing aggregate particles of larger size. The punching shear resistance is given by the following formula

$$V_R(\psi) = \frac{0.75\sqrt{f_c}}{1 + 15\psi d/d_{dg}} b_0 d \tag{2.2}$$

where: f_c – concrete compressive strength, ψ – the slab rotation, d – the effective depth, d_{dg} – parameter describing roughness of the crack, b_0 – length of the control perimeter at the distance of $d/2$ from the column edge.

The parameter d_{dg} in the expression (2.2) describes the roughness of the crack surface, which depends on the maximum size of the aggregate particles used in concrete. As stated by the authors of the papers [8, 13], when determining the d_{dg} parameter, it is reasonable to take into account the influence of concrete compressive strength. This results from the limited aggregate interlock effect in case of high-strength concrete due to breaking and crushing of the aggregate particles [14]

$$d_{dg} = 16 + d_g \cdot \min\left\{\begin{matrix}(60/f_c)^2 \\ 1.0\end{matrix}\right\} \leq 40 \text{ mm} \tag{2.3}$$

where: d_g – the maximum aggregate size, f_c – concrete compressive strength

A similar problem occurs in lightweight concrete, where the aggregate is the weakest component of the composite. Contrary to ordinary concrete, where cracks form at the

www.czasopisma.pan.pl PAN www.journals.pan.pl

interface between the aggregate particles and cement paste, in lightweight concrete breaking of the aggregate particles occurs. This results from a limited crushing resistance of the lightweight aggregate. As a result, the shear surface is characterized by a relatively low roughness, which results primarily from the contribution of natural aggregate particles – if such an aggregate is present. Figure 3 shows the fracture surfaces of ordinary concrete and lightweight aggregate concrete of the density class 1.8. In both concretes, natural sand of the 0÷2 mm graining was used as fine aggregate, while the coarse aggregate of the 2÷8/9 mm graining was granite grit (Fig. 3a) or "Certyd" lightweight aggregate manufactured in the process of fly ash sintering (Fig. 3b).

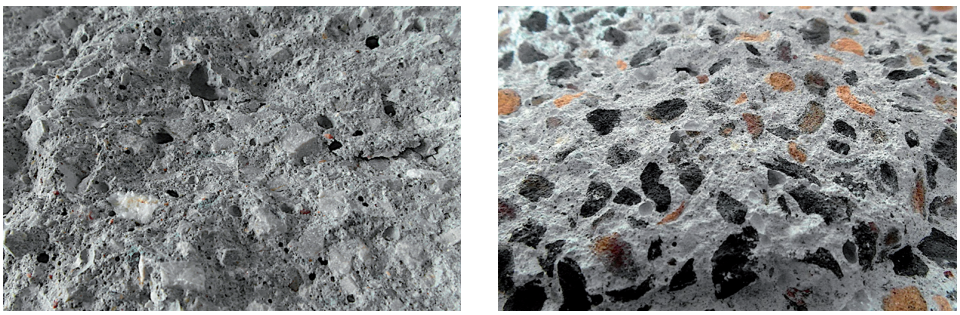

(a) (b)

Fig. 3. View of the breakthrough surface: (a) concrete with natural crushed aggregate, (b) concrete with granulated lightweight aggregate

The effect of the particle size d_g, which determines the interlock effect, is illustrated on the example of the punching shear capacity of a 200 mm thick slab made of concrete with a compressive strength f_{lcm} = 47.9 MPa – see Fig. 4. Curves describing the failure

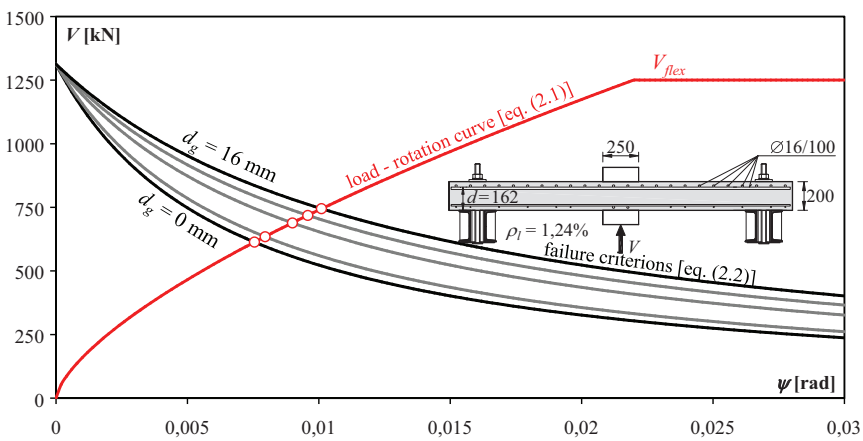

Fig. 4. Effect of the particle size on failure criterion and punching shear capacity

criterions for different aggregate particle sizes d_g ranging from 0 (corresponding to no interlock due to aggregate crushing) to 16 mm were marked with grey and black. The punching shear capacities were determined by considering the intersection of successive curves with the load-rotation curve (red line), which is independent from properties of the aggregate.

Figure 5 shows the change in the punching shear capacity resulting only from the aggregate interlock effect. In the case under consideration, a change in size of the natural aggregate particles from 2 to 16 mm should translate into an increase in the punching shear capacity by about 17%. The omission of natural aggregate in the calculations (which is proposed in the design procedures [5] and [6] based on the CSCT) would result in a slight reduction of the theoretical punching shear capacity by about 3.5%.

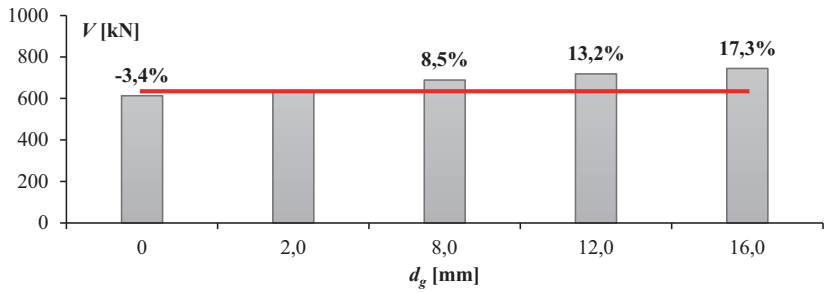

Fig. 5. Effect of particle size on punching shear capacity

3. CSCT in the light of experimental investigations

3.1. Load-rotation response and failure criterion

In order to verify the assumptions related to the limitation of the aggregate interlock contribution, the principles of CSCT were verified in the light of authors' investigations, discussed in more detail in [15–17]. They concerned flat slabs with a thickness of 200 mm and dimensions of 2400 × 2400 mm in plan, made of lightweight concrete with "Certyd" aggregate. This aggregate is a product of fly ash sintering, which is a by-product of hard coal combustion in fine coal boilers in heat and power plants. It is characterized by a bulk density of 700÷900 kg/m^3 (depending on the fraction), crushing resistance above 6 MPa and water absorption after 24 h of about 20%. It allows for production of lightweight structural concretes of 1.8 and 2.0 density classes according to EN 1992-1-1 [4] and compressive strength classes LC20/22÷LC35/38.

All the specimens had the same shape, but different longitudinal reinforcement. Depending on the test series, the longitudinal reinforcement ratio ρ_l ranged from 0.49 to 1.73%. The elements were made from concrete with a mean compressive strength f_{lcm} = 47.9÷52.1 MPa. The theoretical load-rotation curves were determined according to equation (2.1), including the flexural capacity V_{flex} calculated according to yield line theory

(*Elstner* and *Hognestad* [18]). These curves were marked with red in Fig. 6. Blue lines represent the actual load-rotation behaviour and were calculated according to measurements of deformation carried out during the tests.

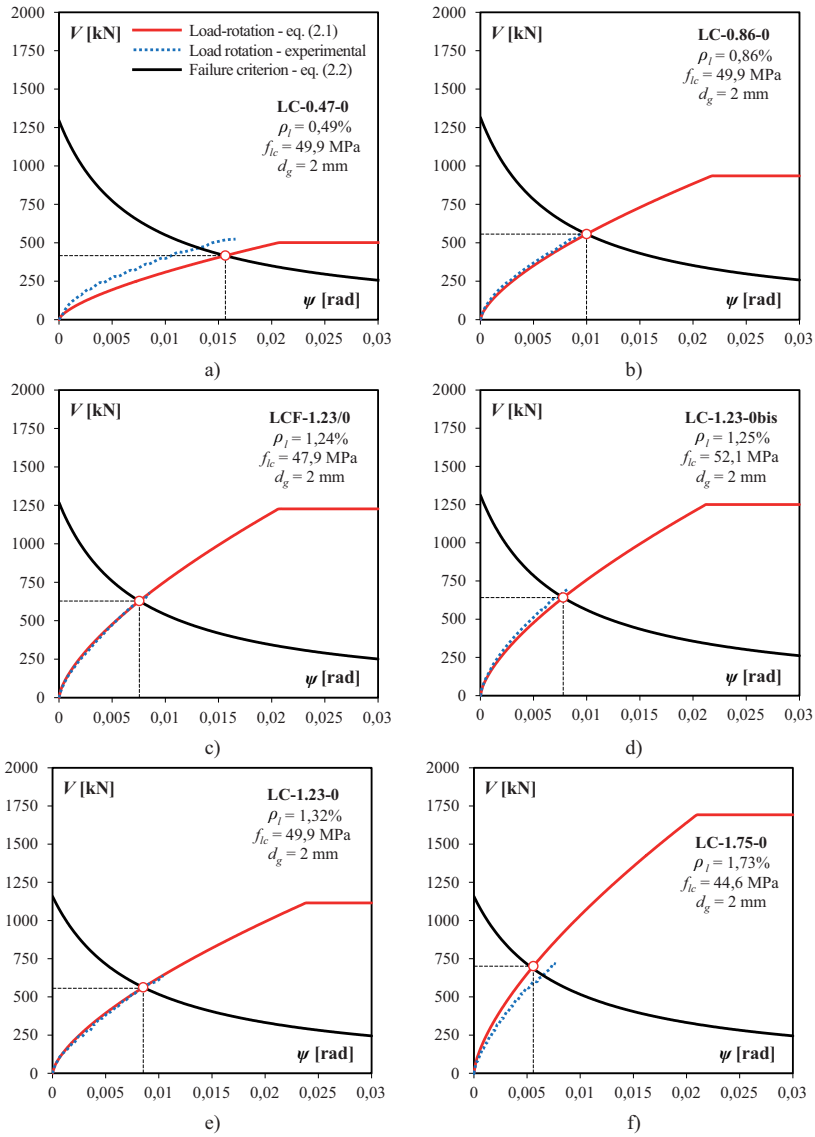

Fig. 6. Load-rotation curves and failure criteria for slabs with various longitudinal reinforcement

A very good agreement between both theoretical and experimental curves can be noticed in case of slabs with the reinforcement ratio $\rho_l = 0.86 \div 1.32\%$. With regard to the LC-0.47-0 specimen ($\rho_l = 0.49\%$), the theoretical rotations at a given load level were up to 50%

higher than the measured ones. On the other hand, in case of LC-1.75-0 slab (ρ_l = 1.73%) the rotations recorded during the test turned out to be higher by about 20÷25%.

The curves describing the failure criterion according to equation (2.2) were marked with black in Fig. 6. The intersection of both red and black curves designates the theoretical punching shear failure. Due to the observed breaking of the lightweight aggregate particles (see Fig. 7), in the calculations only size of the natural aggregate (sand) was taken into account.

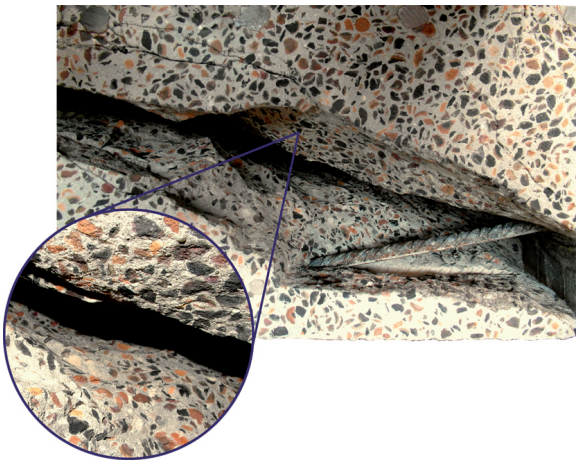

Fig. 7. View of the opened critical shear crack with broken aggregate particles

Figure 8 compares the ultimate rotations recorded immediately before failure of the slabs and values resulting from calculations according to CSCT. It can be seen that the theoretical values were generally lower than the actual ones by a maximum of 24.9% (on average by about 11%). This difference was not found to be dependent on the longitudinal reinforcement ratio. Despite the differences in the ultimate rotations defining failure, the theoretical punching shear capacities resulting from the failure criterion (2.2) turned out to be very close to the experimental loads. The mean ratio of the experimental to theoretical load capacity $V_{\text{exp}}/V_{\text{calc}}$ of 1.10 was obtained with a coefficient of variation of 6.3%. The analysis demonstrated then the usefulness of CSCT for the assessment of the punching shear capacity of flat slabs made from lightweight concrete with "Certyd" aggregate.

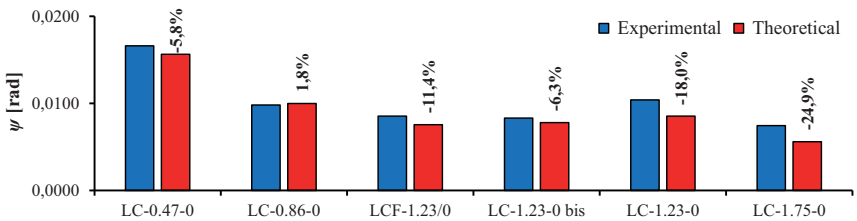

Fig. 8. Comparison between experimental and theoretical rotations of the slabs at failure

3.2. Load carrying capacity

In order to evaluate the CSCT in relation to the slabs made from concrete with also other types of lightweight aggregates, 57 results of the previous experimental investigations were analysed. Apart from the authors' investigations, the following research were included:

- *Youm* et al. [10] – 4 slabs with thickness of 200, 280, 300 mm and dimensions of 2500 × 3000 mm in plane; four different types of lightweight aggregate were used: shale coarse aggregate with crushed shapes (L-SH-C), clay coarse aggregate with spherical (L-CL-S) or partially crushed shapes (L-CL-C) and slate coarse aggregate with crushed shape (L-SL-C), thoroughly cleaned sea-sand as natural fine aggregate of fineness modulus equal to 2.83;
- *Caratelli* et al. [11] – 1 slab with thickness of 200 mm and dimensions of 2400 × 2400 mm in plane; structural expanded clay aggregate LECA (0÷15 mm), sand (0÷4 mm) and coarse aggregate (2÷16 mm) were used;
- *Sun-Kyu* et al. [19] – 2 slabs with thickness of 220 mm and dimensions of 2000 × 3600 mm in plane; lightweight aggregate made by sintering of fly ash, stone powder sludge and clay was used;
- *Tomaszewicz* [20] – 6 slabs with thickness of 120, 240, 320 mm and dimensions of 3000 × 3000, 2600 × 2600, 1500 × 1500 mm in plane; lightweight aggregate Liapor manufactured in a process of burning of raw clay in a rotary oven was used – coarse (4÷8, 8÷16 mm) and fine (0÷8 mm) fractions of the aggregate were included;
- *Osman* et al. [21] – 4 slabs with thickness of 150 mm and dimensions of 1900 × 1900 mm in plane; lightweight aggregate with a maximum particle size of 19 mm was used, produced through thermal expansion of slate in rotary kilns;
- *Clarke* and *Birjandi* [22] – 26 slabs with thickness of 120 mm and diameter of 1540 mm in plane; natural sand and five different types of lightweight aggregates were used: sintered pulverized fuel ash (Lytag), pelletized blast furnace slag (Pellite), expanded clay (LECA), expanded clay (Fibo), expanded shale (Liapor).
- *Mizukoshi* et al. [23] – 8 slabs with thickness of 100, 150 mm and dimensions of 1000 × 1000 mm in plane; river sand (0÷2.5 mm) and artificial lightweight coarse aggregate from expansive shale (0÷15 mm) were used.

The main parameters characterizing the test specimens as well as the selected results of the calculations are summarized in Table 1. The experimental load carrying capacities V_{calc} were estimated considering an intersection of the curves given by equations (2.1) and (2.2), obtained at the theoretical ultimate rotation ψ_{calc}.

The average ratio of the experimental to theoretical load capacity $V_{\mathrm{exp}}/V_{\mathrm{calc}} = 1.06$ was obtained with a relatively low coefficient of variation of 9.1%. Figures 9–11 compare the results of calculations as a function of selected parameters, such as: longitudinal reinforcement ratio ρ_l, concrete compressive strength f_{lc} and concrete density ρ. The equation of the regression line shows that the $V_{\mathrm{exp}}/V_{\mathrm{calc}}$ ratio is almost independent on the reinforcement ratio ρ_l. Only in case of the compressive strength and concrete density, an increase in the $V_{\mathrm{exp}}/V_{\mathrm{calc}}$ ratio resulting from increasing the indicated parameters, is observed. These changes, however, are not particularly significant and increasing the compressive strength f_{lc} from 10 to 75 MPa results in an increase in the $V_{\mathrm{exp}}/V_{\mathrm{calc}}$ ratio by

13%. With regard to the density only slight increase in the V_{exp}/V_{calc} ratio of 9% can be observed by changing the density ρ from 1500 to 2100 kg/m^3.

Table 1. Details of the test specimens included in the comparative analysis

Test	Specimen	f_{lc} [MPa]	f_y [MPa]	ρ [kg/m^3]	ρ_l [%]	d_g [mm]	c/D [mm]	d [mm]	V_{exp} [kN]	ψ_{calc} [rad]	V_{calc} [kN]	$\frac{V_{exp}}{V_{calc}}$
[20]	LWA75-1-1	69.2	500	2007	1.49	8	200	275	1600	0.0037	1511.1	1.06
	LWA75-2-1	70.3	500	1999	1.75	8	150	200	950	0.0042	877.0	1.08
	LWA75-2-1D	74.0	500	2062	1.75	8	150	200	1100	0.0042	887.0	1.24
	LWA75-2-3	74.1	500	2035	2.62	8	150	200	1150	0.0029	1004.3	1.15
	LWA75-2-3D	74.4	500	2052	2.62	8	150	200	1020	0.0029	1005.4	1.01
	LWA75-3-1	68.5	500	2016	1.84	8	100	88	320	0.0067	230.2	1.39
[21]	HSLW0.5P	76.1	450	n/d	0.53	2[1]	250	120	263.8	0.0232	266.7	0.99
	HSLW1.0P	73.4	435	n/d	1.10	2[1]	250	115	414.8	0.0144	348.2	1.19
	HSLW1.5P	75.5	435	n/d	1.66	2[1]	250	115	474.3	0.0106	418.1	1.13
	HSLW2.0P	74.0	435	n/d	2.21	2[1]	250	115	518.0	0.0083	465.8	1.11
[22]	1	20.8	460[2]	1800	0.78	2	140	100	151.0	0.0080	154.5	0.98
	2	21.7	460[2]	1800	1.54	2	140	98	187.0	0.0047	184.9	1.01
	3	28.8	460[2]	1800	1.54	2	140	98	206.0	0.0052	207.0	1.00
	4	27.4	460[2]	1800	0.78	2	140	100	166.0	0.0090	169.6	0.98
	5	50.0	460[2]	1800	0.78	2	140	100	203.0	0.0114	205.3	0.99
	6	57.1	460[2]	1800	1.54	2	140	98	259.0	0.0068	266.3	0.97
	7	29.6	460[2]	2040	1.54	2	140	98	208.0	0.0052	209.4	0.99
	8	29.8	460[2]	2040	0.78	2	140	100	171.0	0.0092	174.3	0.98
	9	23.3	460[2]	2040	0.78	2	140	100	157.0	0.0084	160.5	0.98
	10	13.2	460[2]	2040	0.78	2	140	100	130.0	0.0068	130.8	0.99
[22]	11	10.6	460[2]	2040	1.54	2	140	98	148.0	0.0041	134.3	1.10
	12	41.8	460[2]	2040	0.78	2	140	100	191.0	0.0106	194.2	0.98
	13	46.6	460[2]	2040	1.54	2	140	98	241.0	0.0063	247.9	0.97
	14	24.0	460[2]	1665	0.78	2	140	100	159.0	0.0085	162.2	0.98
	15	23.9	460[2]	1665	1.54	2	140	98	193.0	0.0049	192.3	1.00
	16	18.3	460[2]	1665	0.78	2	140	100	145.0	0.0077	147.5	0.98
	17	18.6	460[2]	1665	1.54	2	140	98	178.0	0.0045	173.6	1.03
	18	23.4	460[2]	1510	0.78	2	140	100	157.0	0.0084	160.9	0.98
	19	20.7	460[2]	1510	1.54	2	140	98	184.0	0.0046	181.3	1.01
	20	17.0	460[2]	1510	0.78	2	140	100	142.0	0.0075	143.9	0.99

Continued on next page

Table 1 [cont.]

Test	Specimen	f_{lc} [MPa]	f_y [MPa]	ρ [kg/m^3]	ρ_l [%]	d_g [mm]	c/D [mm]	d [mm]	V_{exp} [kN]	ψ_{calc} [rad]	V_{calc} [kN]	$\frac{V_{exp}}{V_{calc}}$
	21	22.6	460[2]	1565	0.78	2	140	100	155.0	0.0083	158.8	0.98
	22	22.3	460[2]	1565	1.54	2	140	98	189.0	0.0047	187.0	1.01
	23	32.8	460[2]	1565	0.78	2	140	100	176.0	0.0096	179.8	0.98
	24	30.5	460[2]	1565	1.54	2	140	98	210.0	0.0053	211.8	0.99
	25	45.9	460[2]	1945	0.78	2	140	100	197.0	0.0110	199.9	0.99
	26	42.1	460[2]	1945	1.54	2	140	98	234.0	0.0060	238.9	0.98
[10]	L-SH-C	37.2	411	1898	0.24	2	300	180	552	0.0128	499.1	1.11
	L-CL-S	34.2	411	1847	0.24	2	300	180	626.3	0.0124	488.3	1.28
	L-CL-C	45.6	411	2059	0.16	2	300	260	929	0.0105	812.6	1.14
	L-SL-C	46.7	411	1816	0.15	2	300	280	784.2	0.0100	893.8	0.88
[19]	LS-1	47.4	400	1895	0.52	2	200×500	180	669	0.0118	660.2	1.01
	LS-2	47.4	400	1895	0.52	2	200×500	180	702	0.0118	660.2	1.06
[23]	LC-1	41.3	391	1810	1.14	2.5	100	75	136.2	0.0093	127.6	1.07
	LC-2	41.3	391	1810	0.76	2.5	100	75	123	0.0133	110.3	1.12
	LC-3	38.7	391	1840	0.81	2.5	100	105	236	0.0074	194.2	1.22
	LC-4	38.7	391	1840	0.54	2.5	100	105	193.9	0.0106	166.6	1.16
	LC-1’	41.3	391	1810	1.14	2.5	100	75	136.6	0.0093	127.6	1.07
	LC-2’	41.3	391	1810	0.76	2.5	100	75	123	0.0133	110.3	1.12
	LC-3’	38.7	391	1840	0.81	2.5	100	105	234.7	0.0074	194.2	1.21
	LC-4’	38.7	391	1840	0.54	2.5	100	105	195	0.0106	166.6	1.17
[16]	LC-0.47-0	49.9	537.7	1780	0.49	2	250	162	520	0.0155	419.4	1.24
	LC-0.86-0	49.9	578.8	1780	0.86	2	250	164	590	0.0098	562.5	1.05
	LC-1.23-0	49.9	578.8	1780	1.32	2	250	149	640	0.0082	575.0	1.11
[17]	LC-1.75-0	44.6	547.7	1695	1.73	2	250	163	720	0.0056	703.8	1.02
[15]	LC-1.23-0 bis	52.1	547.7	1788	1.25	2	250	161	700	0.0078	643.2	1.09
–	LCF-1.23/0	47.9	536.7	1799	1.24	2	250	162	680	0.0075	629.7	1.08
[11]	L-MSW	58.6	520	2064	1.66	16	400	150	862	0.0104	860.7	1.00

f_{lc} – compressive strength of LWAC, f_y – yield strength of the reinforcement, ρ – concrete density, ρ_l – reinforcement ratio, d_g – particle size of the natural aggregate, c/D – column size, d – effective depth, V_{exp} – experimental load, ψ_{calc} – slab rotation, V_{calc} – theoretical load capacity.

[1] The diameter of the natural sand particles was not given – the value was assumed as in typical cases.
[2] Yield strength assumed according to previous investigations described in [24].

The low sensitivity to the change of the indicated parameters in a fairly wide range allows to conclude that the CSCT satisfactorily describes the punching shear capacity of slabs made from various types of lightweight aggregate concretes.

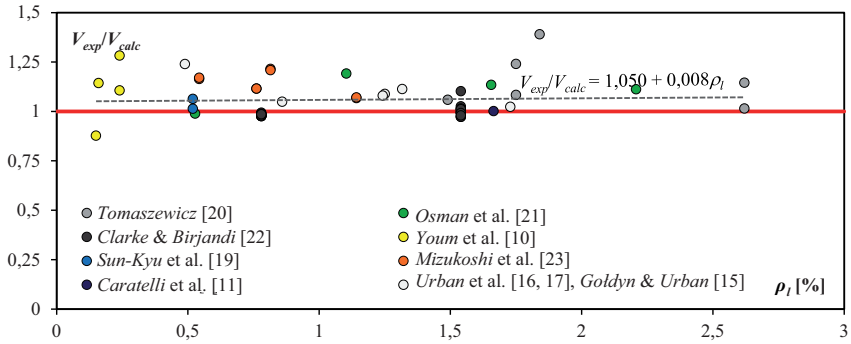

Fig. 9. Relation between experimental and theoretical punching shear capacity depending on longitudinal reinforcement ratio

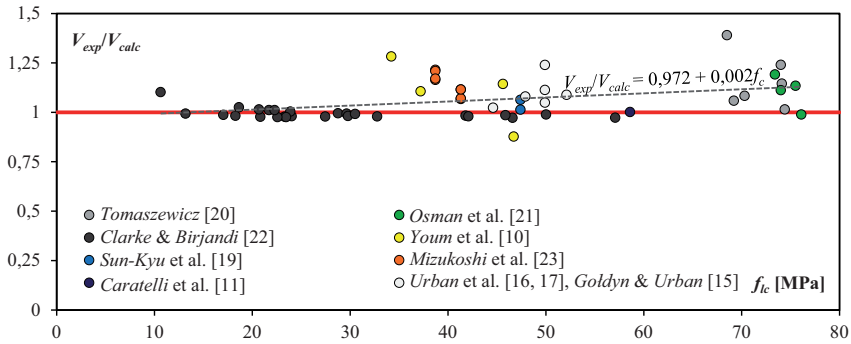

Fig. 10. Relation between experimental and theoretical punching shear capacity depending on concrete compressive strength

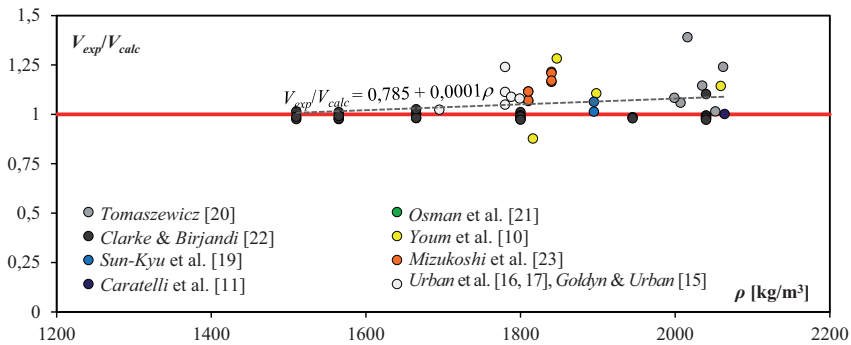

Fig. 11. Relation between experimental and theoretical punching shear capacity depending on concrete density

www.czasopisma.pan.pl PAN www.journals.pan.pl
POLSKA AKADEMIA NAUK

4. Conclusions

The analysis of the results of experimental tests in the light of CSCT allowed to state a good compliance of the adopted mechanical model with the actual behavior of lightweight aggregate concrete slabs. The assumed load-rotation function allowed to describe the deformations of the lightweight concrete slabs with aggregate from sintered fly ash in a qualitatively and quantitatively satisfactory manner. The theoretical ultimate rotations turned out to be on average about 11% lower than the values recorded during the authors' tests.

One of the key issues by formulating the failure criterion is the determination of the effective roughness of the failure surface, which affects the aggregate interlock effect. Due to the mechanical properties of lightweight aggregate (limited crushing strength and thus high susceptibility to breaking), its contribution to the interlock effect was omitted in the analysis. On the other hand, the maximum size of natural aggregate particles was included, which allowed for a very good agreement between the results of calculations and the experimental loads. The results of the tests on 57 flat slabs made from various types of lightweight aggregate concretes were analyzed, obtaining an average ratio of the experimental to theoretical load of 1.06, with a coefficient of variation of 9.1%. The performed parametric study showed a low sensitivity of correctness of the CSCT predictions to a change in a fairly wide range of parameters such as longitudinal reinforcement ratio, concrete compressive strength and density of lightweight aggregate concrete.

References

[1] M.N. Haque, H. Al-Khaiat, and O. Kayali, "Strength and durability of lightweight concrete", *Cement and Concrete Composites*, vol. 26, no. 4, pp. 307–314, 2004, DOI: 10.1016/S0958-9465(02)00141-5.

[2] C.L. Roberts-Wollmann, T. Banta, R. Bonetti, and F. Charney, "Bearing strength of lightweight concrete", *ACI Materials Journal*, vol. 103, no. 6, pp. 459–466, 2006, DOI: 10.14359/18224.

[3] J.A. Bogas and R. Nogueira, "Tensile strength of structural expanded clay lightweight concrete subjected to different curing conditions", *KSCE Journal of Civil Engineering*, vol. 18, no. 6, pp. 1780–1791, 2014, DOI: 10.1007/s12205-014-0061-x.

[4] EN 1992-1-1 EN 1992-1-1: Eurocode 2: Design of concrete structures – Part 1–1: General rules and rules for buildings. Brussels: European Committee for Standardisation, 2004.

[5] *fib Bulletin 66. Model Code 2010 – Final draft,* vol. 2. 2012.

[6] CEN, prEN 1992-1-1 Eurocode 2: Design of concrete structures – Part 1–1: General rules — Rules for buildings, bridges and civil engineering structures. 2021.

[7] A. Muttoni, "Punching shear strength of reinforced concrete slabs without transverse reinforcement", *ACI Structural Journal*, vol. 105, no. 4, pp. 440–450, 2008, DOI: 10.14359/19858.

[8] A. Muttoni, M. Fernández Ruiz, and J. Simões, "Recent improvements of the Critical Shear Crack Theory for punching shear design and its simplification for code provisions", in *fib Congress 2018. Better, Smarter, Stronger.* Melbourne, 2018, pp. 1–10.

[9] S. Kinnunen and H. Nylander, *Punching of concrete slabs without shear reinforcement*. Göteborg: Royal Institute of Technology, 1960, no. 158.

[10] K.S. Youm, J.J. Kim, and J. Moon, "Punching shear failure of slab with lightweight aggregate concrete (LWAC) and low reinforcement ratio", *Construction and Building Materials*, vol. 65, pp. 92–102, 2014, DOI: 10.1016/j.conbuildmat.2014.04.097.

[11] A. Caratelli, S. Imperatore, A. Meda, and Z. Rinaldi, "Punching shear behavior of lightweight fiber reinforced concrete slabs", *Composites Part B: Engineering*, vol. 99, pp. 257–265, 2016, DOI: 10.1016/j.compositesb.2016.06.045.

[12] A. Muttoni and J. Schwartz, "Behaviour of beams and punching in slabs without shear reinforcement", in *IABSE Colloquium*, vol. 62, pp. 703–708, 1991, DOI: 10.5169/seals-47705.

[13] A. Muttoni, M. Fernández Ruiz, and J. T. Simões, "The theoretical principles of the critical shear crack theory for punching shear failures and derivation of consistent closed-form design expressions", *Structural Concrete*, vol. 19, no. 1, pp. 174–190, 2018, DOI: 10.1002/suco.201700088.

[14] E.G. Sherwood, E.C. Bentz, and M.P. Collins, "Effect of aggregate size on beam-shear strength of thick slabs", *ACI Structural Journal*, vol. 105, no. 1, pp. 115–116, 2008.

[15] M. Gołdyn and T. Urban, "Hidden Capital as an Alternative Method for Increasing Punching Shear Resistance of LWAC Flat Slabs", *Archives of Civil Engineering*, vol. 65, no. 4, pp. 309–328, 2019, DOI: 10.2478/ace-2019-0062.

[16] M. Gołdyn, Ł. Krawczyk, W. Ryżyński, and T. Urban, "Experimental Investigations on Punching Shear of Flat Slabs Made from Lightweight Aggregate Concrete", *Archives of Civil Engineering*, vol. 64, no. 4, pp. 293–306, 2018, DOI: 10.2478/ace-2018-0058.

[17] T. Urban, M. Gołdyn, Ł. Krawczyk, and Ł. Sowa, "Experimental investigations on punching shear of lightweight aggregate concrete flat slabs", *Engineering Structures*, vol. 197, art. no. 109371, 2019, DOI: 10.1016/j.engstruct.2019.109371.

[18] R.C. Elstner and E. Hognestad, "Shearing Strength of Reinforced Concrete Slabs", *ACI Journal Proceedings*, vol. 53, no. 7, pp. 29–58, 1956.

[19] C. Sun-Kyu, J.-W. Kwark, J.-M. Lee, and Dae-Joong-Moon, "Punching Shear Behavior of High-strength Lightweight Concrete Slab Under Concentrated Load", *KSCE Journal of Civil and Environmental Engineering Research*, vol. 26, no. 1A, pp. 219–228, 2006.

[20] A. Tomaszewicz, *High Strength Concrete: SP2 – Plates and Shells Report 2.3. Punching Shear Capacity of Reinforced Concrete Slabs. SINTEF Report No. STF70 A93082*. SINTEF, 1993.

[21] M. Osman, H. Marzouk, and S. Helmy, "Behavior of high-strength lightweight concrete slabs under punching loads", *ACI Structural Journal*, vol. 97, no. 3, pp. 492–498, 2000, DOI: 10.14359/4644.

[22] J.L. Clarke and F.K. Birjandi, "Punching shear resistance of lightweight aggregate concrete slabs", *Magazine of Concrete Research*, vol. 42, no. 152, pp. 171–176, 1990, DOI: 10.1680/macr.1990.42.152.171.

[23] M. Mizukoshi, S. Matsui, and H. Higashiyama, "Punching shear strength of RC slabs using lightweight concrete", in *Challenges, Opportunities and Solutions in Structural Engineering and Construction*, N. Ghafoori, Ed. CRC Press, 2009, pp. 111–118.

[24] J.L. Clarke, "Shear strength of lightweight aggregate concrete beams: Design to BS 8110", *Magazine of Concrete Research*, vol. 39, no. 141, pp. 205–213, 1987, DOI: 10.1680/macr.1987.39.141.205.

Zastosowanie teorii krytycznej rysy ukośnej do określania nośności na przebicie płyt wykonanych z lekkich betonów kruszywowych

Słowa kluczowe: rozmiar ziaren, przebicie, lekki beton kruszywowy, zazębianie kruszywa, Critical Shear Crack Theory

Streszczenie:

Jednym z podstawowym problemów przy projektowaniu stropów płaskich z lekkich betonów kruszywowych jest zapewnienie odpowiedniej nośności na przebicie stref podporowych. Mimo niewątpliwych zalet, do których można zaliczyć mniejszy ciężar objętościowy czy też lepsze właściwości izolacyjne, lekkie betony kruszywowe charakteryzują się mniejszą o 10 do nawet ponad 30% wytrzymałością na rozciąganie w porównaniu z betonami zwykłymi o zbliżonej wytrzymałości na

www.czasopisma.pan.pl PAN POLSKA AKADEMIA NAUK www.journals.pan.pl

ściskanie. W odróżnieniu od obowiązującej obecnie normy EN 1992-1-1, bazującej na formułach pół-empirycznych, za podstawę określania nośności płyt na przebicie w procedurach *fib* Model Code 2010 i prEN 1992-1-1 przyjęto podejście mechaniczne, nawiązujące do Teorii Krytycznej Rysy Ukośnej (*Critical Shear Crack Theory* – CSCT). Teoria ta zakłada, że wskutek powstania rys ukośnych, mechanizm przenoszenia sił poprzecznych staje się zależny głównie od efektu zazębiania kruszywa, resztkowej wytrzymałości betonu na rozciąganie, oporu ścinania betonu w strefie ściskanej oraz mechanizmu dyblującego zbrojenia głównego. Nośność na przebicie została powiązana ze zdolnością płyty do deformacji, reprezentowanej w przypadku płyt smukłych przez kąt obrotu ψ, który może zostać wyrażony jako całka z krzywizny płyty w rozważanej strefie.

Procedura obliczeniowa CSCT, nie wyróżnia wyraźnie zasad projektowania na przebicie płyt z lekkich betonów kruszywowych, jak ma to miejsce w normie EN 1992-1-1. Zakłada się, że deformacje płyty zarysowanej są powiązane przede wszystkim z jej przekrojem (wysokością użyteczną) i zastosowanym zbrojeniem podłużnym a zatem powinny opisywać zachowanie zarówno płyt z betonu zwykłego jak i lekkiego. W celu określenia nośności na przebicie konieczne jest rozważanie kryterium zniszczenia opisanego pół-empiryczną formułą, w której nośność została uzależniona od szerokości rysy ukośnej, powiązanej z kątem obrotu płyty. Uwzględnia ono efekt zazębiania kruszywa, który jest zależny od profilu powierzchni rysy ukośnej. Rozmiar ziaren warunkuje szorstkość powierzchni, dlatego też przy jednakowej szerokości rysy większego efektu zazębiania kruszywa, odpowiedzialnego za przenoszenie sił stycznych, należy oczekiwać w przypadku betonu zawierającego ziarna kruszywa o większej średnicy. Istotny problem w przypadku lekkich betonów kruszywowych stanowi ograniczona wytrzymałość na miażdżenie kruszywa lekkiego. W odróżnieniu od betonu zwykłego, w którym rysy formują się na styku ziaren i zaczynu, w betonie lekkim dochodzi do pękania ziaren, skutkiem czego powierzchnia rysy ukośnej charakteryzuje się stosunkowo niedużą chropowatością. Biorąc pod uwagę obserwacje z badań własnych, można stwierdzić, że profil powierzchni zależny jest wówczas przede wszystkim od uziarnienia kruszywa naturalnego, które nie ulega pękaniu i umożliwia zazębianie ziaren. W świetle CSCT wskutek zastąpienia części kruszywa naturalnego kruszywem lekkim należy oczekiwać niższej o kilka do kilkunastu procent nośności płyty na przebicie, w zależności od uziarnienia pozostałej frakcji kruszywa naturalnego.

W celu oceny założeń związanych z ograniczonym zazębianiem kruszywa, dokonano weryfikacji zasad CSCT w świetle badań własnych. Obejmowały one płyty płaskie o grubości 200 mm i wymiarach w rzucie 2400×2400 mm, wykonane z lekkiego betonu na kruszywie "Certyd", stanowiącym produkt spiekania popiołów lotnych. Elementy wykonano z betonu o wytrzymałości na ściskanie $f_{\mathrm{lcm}} = 47,9 \div 52.1$ MPa, natomiast stopień zbrojenia głównego ρ_l, w zależności od serii badawczej, wynosił od 0,49 do 1,73%. W przypadku płyt charakteryzujących się stopniem zbrojenia głównego $\rho_l = 0,86 \div 1,32\%$ uzyskano bardzo dobrą zgodność pomiędzy teoretycznymi i eksperymentalnymi zależnościami obciążenie-obrót, zarówno pod względem jakościowym jak i ilościowym. Jedynie w odniesieniu do dwóch elementów zauważalne były różnice pomiędzy rzeczywistą i przewidywaną charakterystyką obciążenie-deformacja. W przypadku płyty LC-0.47-0 ($\rho_l = 0,49\%$) teoretyczne kąty obrotu przy danym poziomie obciążenia były do 50% większe od wartości pomierzonych, natomiast w przypadku modelu LC-1.75-0 ($\rho_l = 1,73\%$) większe o około $20 \div 25\%$ okazały się kąty obrotu zarejestrowane w trakcie badania. Graniczne kąty obrotu zarejestrowane bezpośrednio przed zniszczeniem płyt okazały się średnio o około 11% niższe od wartości teoretycznych, wynikających z obliczeń według CSCT. Maksymalna różnica nie przekraczała 24,9%. Nie stwierdzono przy tym, by była ona zależna była od stopnia zbrojenia głównego. Mimo różnic w granicznych kątach obrotów teoretyczne nośności na przebicie wynikające z kryterium zniszczenia okazały się bardzo zbliżone do wartości eksperymentalnych. Uzyskano średni stosunek nośności eksperymentalnej do teoretycznej $V_{\mathrm{exp}}/V_{\mathrm{calc}}$ równy 1,10 przy współczynniku zmienności na poziomie 6,3%.

www.czasopisma.pan.pl PAN POLSKA AKADEMIA NAUK www.journals.pan.pl

W pracy przeanalizowano również dostępne w literaturze wyniki badań 57 płyt płaskich wykonanych z różnych rodzajów betonów, w których stosowano sztuczne kruszywo lekkie powstałe w procesie wypalania łupków, surowej gliny, popiołów lotnych a także granulowany żużel wielopiecowy i keramzyt. Ze względu na właściwości mechaniczne kruszywa lekkiego (ograniczoną wytrzymałość na miażdżenie i tym samym podatność na pękanie) w analizie pominięto jego udziałw efekcie zazębiania. Uwzględniono natomiast maksymalny wymiar ziaren kruszywa naturalnego, co pozwoliło na uzyskanie bardzo dobrej zgodności pomiędzy wynikami obliczeń a nośnościami eksperymentalnymi płyt. Otrzymano bowiem średni stosunek nośności eksperymentalnej do teoretycznej równy 1,06, przy współczynniku zmienności na poziomie 9,1%. Przeprowadzona analiza parametryczny wykazała niewielką wrażliwość przewidywań CSCT na zmianę w dość szerokim zakresie takich parametrów jak stopień zbrojenia podłużnego ρ_l, wytrzymałość na ściskanie f_{lc} oraz gęstość lekkiego betonu kruszywowego ρ. Wykazano tym samym przydatność CSCT do oceny nośności na przebicie płyt płaskich z lekkiego betonu kruszywowego.

Received: 2022-03-24, Revised: 2022-06-21